Inspection and Analysis of ancient Monastery of "São Romão de Neiva", Portugal

Jahdiel Villafuerte[1], Johann Arias[2], Cindy Calbimonte[3], Jorge Scaff[4], Graça Vasconcelos[5], and Francisco Fernandes[6]

Abstract. The monastery of São Romão de Neiva is an ancient building located in the north of Portugal, in the district of Viana do Castelo and it is considered to be of national interest by the Portuguese Institute of Monuments (DGPC). Due to its importance, an inspection to identify damages and their causes was performed on this building. The inspection and diagnosis included a historical, geometrical and defects survey, and mechanical and physical characterization of the masonry stone. Non-destructive tests on the structural elements such as GPR and sonic tests were also carried out to assess the internal morphology of the stone masonry walls and estimate the quality and modulus of elasticity, respectively. Qualitative assessment of masonry walls using the MQI (Masonry Quality index) was also carried out. Finally, by means of a visual inspection of the structure, the assessment of the damages and pathologies on the structural elements was performed. This **work focus on** the most important **experimental results** and some recommendations to apply them on a structural analysis.

Keywords: Inspection and diagnosis, Visual Inspection, Historical Survey, Damage and Pathology, Geometrical survey, Non-destructive test, Qualitative assessment.

1 Introduction

The Monastery of São Romão de Neiva was part of an ensemble of Benedictine monasteries founded as the result of the spreading of the São Bento Order along the Iberic Penninsula [1] and its relationship with the route to Santiago de Compostela. This monastery is located in the north or Portugal in the town of São Romão de Neiva, which belongs to the Freguesia de Neiva of the Municipal Chamber of Viana do Castelo. The geographical setting denotes a rural landscape with agricultural fields which was the principal activity of the Benedictines.

The main objective of this paper is to present the works carried out in the inspection and diagnosis of the building. These works were performed to characterize the structural system and materials as well to identify and localize the main pathologies. The results of the tests might be useful to carry out the structural analysis and seismic assessment of monastery.

[1] Master Student, Department of Civil Engineering, University of Minho, Guimarães, Portugal, jahdiel1634@gmail.com
[2] Master Student, Department of Civil Engineering, University of Minho, Guimarães, Portugal, johann.milar.arias@gmail.com
[3] Master Student, Department of Civil Engineering, University of Minho, Guimarães, Portugal, cindylu2@gmail.com
[4] Master Student, Department of Civil Engineering, University of Minho, Guimarães, Portugal, jorge-scaff@hotmail.com
[5] Associate Professor, Department of Civil Engineering, ISISE, University of Minho, Guimarães, Portugal, graca@civil.uminho.pt
[6] Associate Professor, Department of Civil Engineering, ISISE, University of Minho, Guimarães, Portugal, fmcpf@civil.uminho.pt

2 The ancient monastery of São Romão de Neiva

The Monastery of São Romão de Neiva was built between the 17th and 19th centuries following several construction stages [1]. The construction phases can be roughly described based on some existing documents as show in the Figure 1. There was a previous Romanic church before the 10th century, of which there is not any actual evidence. A second phase in the 17th century was associated to the demolition of the Romanic church to build a Romanic monastery with baroque style following the concepts of the Tibães mother monastery. A third phase in the 18th century was related to the extension of the monastery. A fourth phase in the 19th century, in the year 1882 was associated with the expulsion of all religion orders in Portugal. One of the bell towers of the church was left incomplete, and in 1894 a fire was registered in the building. Finally, a fifth phase in the 20th century associated to the privatization of the monastery building.

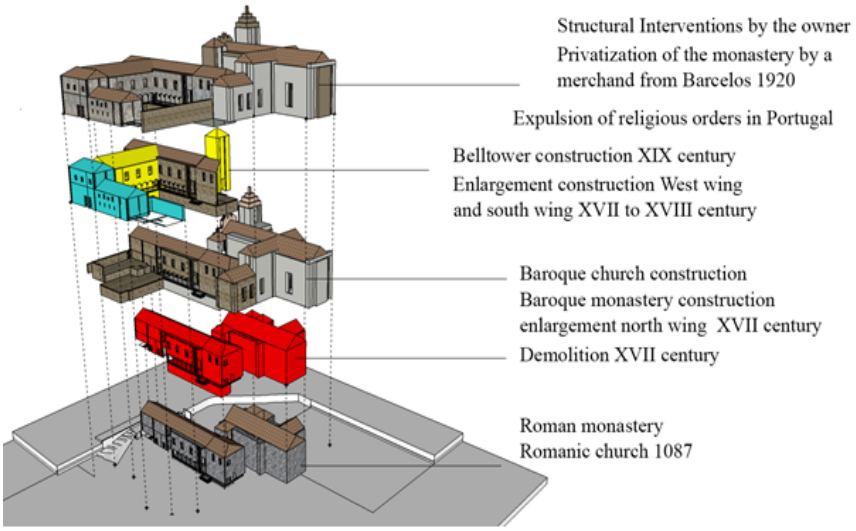

Figure 1: Constructive phases São Romão de Neiva monastery and church complex

2.1 Architectonical and structural description

The monastery is located in the south side of the church. Geometrically it is constituted by 3 sectors arranged in a "U" setting: the north wing, the west wing and the south wing. The typical closed configuration characteristic of Benedictine monasteries was not completed. The complex has a rectangular form of approximately 30 m x 42 m with a central court that opens to the east side. The architectural distribution of spaces and the 3 sectors are presented in Figure 2.

The identification of the most important elements, the connections between the elements and the visual characterization of the material is shown in Figure 3. The system is formed by granite stone masonry bearing walls (Figure 3a), wooden beams bear a wooden boarding floor (Figure 3a). On the inner corridors granite arcade and stone pillars can be observed (Figure 3b). There are three vaults made of brick under the wooden floor (Figure 3c). While the roof was made of wooden trusses and ceramic tiles floor (Figure 3d).

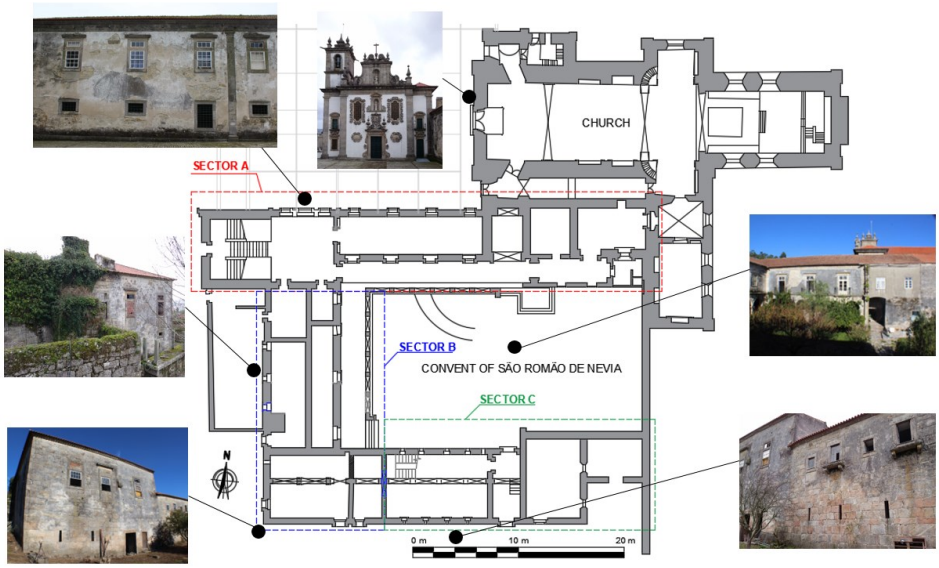

Figure 2: Plan of the monastery of São Romão de Neiva

(a) (c) (c) (d)

Figure 3: Structural typologies. a) Masonry walls and wooden floors. b) Granite stone pillars. c) Brick vaults. d) Wooden trusses.

3 Inspection and diagnosis

The identification of the damages was carried out by visual inspection to map the main damages, and to identify the different materials and structural forms. The origin of the damages was diverse, it is possible that mechanic and environmental effects, and past interventions would have been the main cause. The defects found in the monastery are shown in detail in Figure 4, in accordance with the ICOMOS recommendations [2].

Cracks along the vaults and vertical cracks on one of the walls were identified as shown in Figure 5a, probably these cracks were due to deformation and displacements caused by compression and bending. Other cracks were related to non-structural causes, like material incompatibility between old and new materials such as the addition of cement mortar over the masonry walls (Figure 5b). The damage of higher impact identified was the collapse of timber structural elements (Figure 5c): the wooden beam floors, especially in the west wing of the building and the wooden trusses. The collapse might be related to overloading in some of floors and to the lack of roof in the west side sector, allowing rainwater infiltrations which led biological colonization on these elements (Figure 5d).

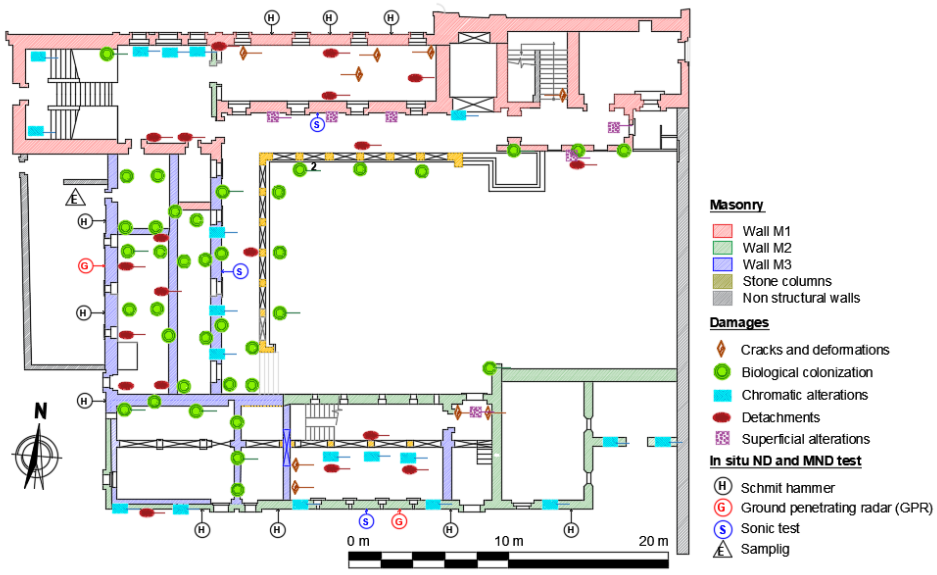

Figure 4: Typologies of masonry walls, mapping damages and an ND & MDT in situ test

(a) (b) (c) (d)

Figure 5: Damages. a) Cracks along the vault. b) Superficial alterations. c). Collapse of structural elements. d) Biologic colonization

It would be recommendable to build a drainage system around the building, in order to collect rainwater and avoid the upward humidity that affects the structure in some localized areas. It is also important to carry out the removal of the biological material present throughout the structure.

3.1 Masonry Quality Index (MQI)

This method proposed by Borri et al [3], consists on the visual assessment of certain parameters to characterize the masonry walls, namely the mechanical properties of bricks or stone (SM), the stone/brick dimensions properties (SD), the stone/brick shape (SS), the classification of the type of connections (WC), vertical joints (VJ), horizontal joints (HJ), mechanical properties of the mortar of joint (MM) and load action to which the masonry wall is subjected. A numerical value is associated to each parameter depending if it complies or not the criteria. Finally, the MQI index is calculated as proposed in equation (1):

$$MQI = SM(SD + SS + WC + HJ + VJ + MM) \quad \textbf{(1)}$$

The calculation was carried out taking into consideration the behavior of the walls when subjected to vertical loads (V) for three types of walls as shown in Figure 4. The highest value of MQI corresponds to category A wall indicating a good behavior for regular masonry. The medium quality masonry corresponds to category B,

an appropriate behavior, with semi-regular masonry. The worse quality is associated to category C (irregular masonry), characterizing a masonry with poor mechanical behavior for vertical loads. Table 1 shows the MQI values and the corresponding categorization for the three types of walls.

Table 1: MQI calculation for masonry walls

Wall	Load	SM	SD	SS	WC	HJ	VJ	MM	MQI	CAT
M1	Vertical (V)	F = 1	F = 1	PF = 1.5	NF = 0	NF = 0	NF = 0	NF = 0	2.5	C
M2	Vertical (V)	F = 1	F = 1	PF = 1.5	PF = 1	NF = 0	PF = 0.5	PF = 0.5	4.5	B
M3	Vertical (V)	F = 1	PF = 0.5	F = 3	PF = 1	F = 2	F = 1	F = 2	9.5	A

4 In situ ND and MDT test

4.1 Schmidt hammer tests

The Schmidt hammer method helped to identify the superficial hardness of the granite stones. The test was carried out on the exterior and interior walls of the monastery, making 10 measurements with 3 repetitions. A Schmidt hammer (NR) to concrete was used in this study, and to calculate the number of rebound correspondent to a hammer (RL) for stone, a correlation was made according to the relationship proposed by H. Viles & A. Goudie [4], Poole & Farmer [4] and A. Aydin [5]. Finally, to estimate the mechanical properties of the stone as a function of the blows of the hammer, such us the density (ρ), the compression strength (UCS) and the young's modulus (E), the correlations proposed by O. Katz & Z. Reches [6] were used. The results of this test are showed in Figure 6, where is presented the average values and the coefficient of variation by each estimated parameter.

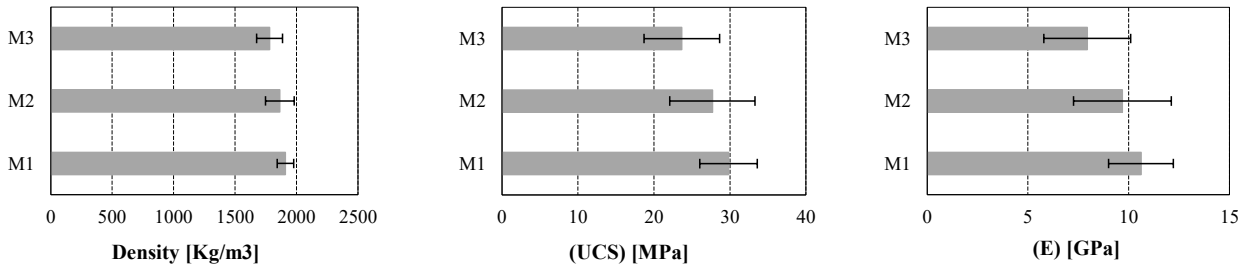

(a) (b) (c)

Figure 6: Parameters obtained with the Schmidt hammer test (a) density, (b) compression strength and (c) young's modulus

4.2 Ground penetrating radar (GPR)

The GPR test was performed to estimate the thickness and the internal morphology of the masonry walls, using an antenna of 800 MHz with an EM wave velocity of 12.5 cm/ns. Two tests were carried in the south (M2) and west (M3) side of the monastery (see Figure 4). Figure 7a shows the scanning on the wall M3, and Figure 7b shows the radargrams of the scan of the wall M2, allowing identify the exterior and interior layer with 25 cm and 55 cm of thickness respectively. On the other hand, for the wall M3 the exterior and interior layer were a

thickness of 30 cm and 50 cm respectively (see Figure 7c). Measurements on the wall M1 did not result in any legible information since the high humidity level did not allow for any reflection.

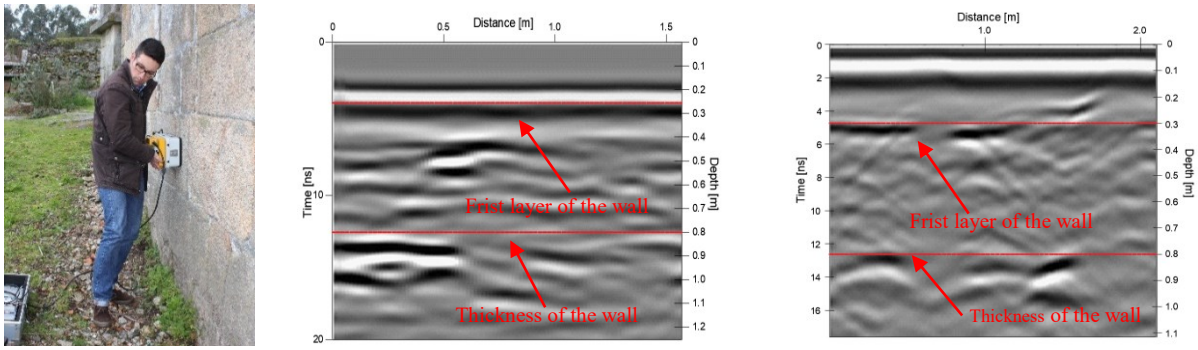

(a) (b) (c)

Figure 7: GPS test. a) Horizontal Scanning. b) Longitudinal radiogram wall M2. c) Longitudinal radiogram wall M3.

4.3 Sonic tests

Sonic test was performed in the three different types of masonry walls as shown in Figure 4. Direct and indirect test (see Figure 8a) were undertaken in order to determine the internal configuration of the walls and stones and to estimate the mechanical properties of the masonry. The results of the direct test average of the VP (primary wave) in all the walls was 1009.4 m/s (CV=16%).The test were carried out over a surface in a grid of points, separated from each other by random separation between 0.40 m to 0.60 cm as show in Figure 8c. Some velocities registered the walls were lower than 700 m/s, probably due to presence of holes inside the masonry configuration (see Figure 8b). In the indirect tests, the VP and VR (Rayleigh wave) were also calculated to estimate the estimate the Elasticity Modulus (E) and the Poisson coefficient (v) for each wall, the volumetric mass (ρ) was adopted of [7]. Table 2 shows the estimated mechanical properties of the walls types tested, the wall M3 is one that presents the highest value of Young's modulus

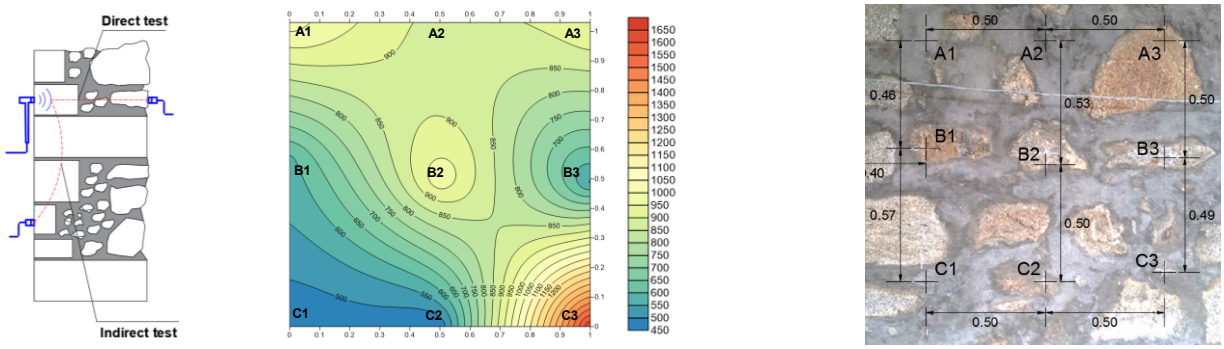

(a) (b) (c)

Figure 8: Sonic test. a) Direct and indirect sonic test, (b) Curves of wave velocities, wall M1. c) Location of the test points wall M1

Table 2: Estimated results of sonic test

Type of Wall	M1	M2	M3
Volumetric density (ρ) – [kg/m^3]	1900	2000	2000
Young's modulus (E_d) – [MPa]	1560 (36%)	2190 (31%)	2300 (16%)
Poisson ratio (ν)	0.263 (20%)	0.284 (27%)	0.209 (12%)

5 Laboratory test

Stone samples were taken from the east side of the monastery (see Figure 4) to perform physical and mechanical test in laboratory tests to characterize granite stone. In Figure 9a the three obtained specimens are shown. The following laboratory tests were carried out: porosity and natural density, absorption by atmospheric pressure, (see Figure 9b). Capillarity, ultrasound test, (see Figure 8c), compression strength and young's modulus (see Figure 8d).

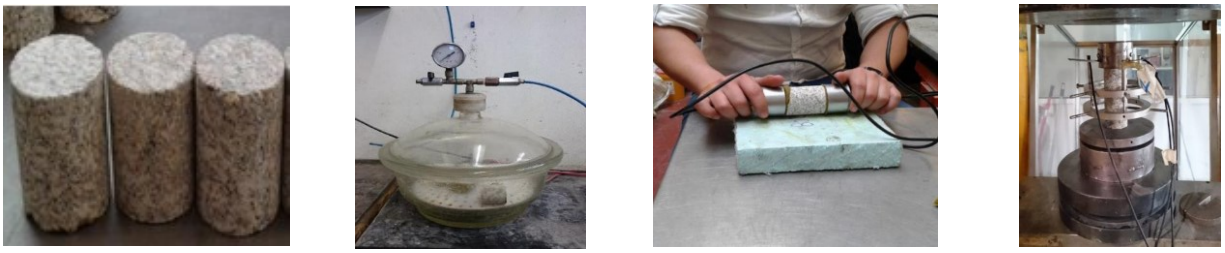

(a) (b) (a) (d)

Figure 9: Laboratory test. a) Specimens. b) Absorption. c) Ultrasonic test. (h) Compression strength and young modulus.

Table 3 shows the results of laboratory tests for the stone's specimens with average values and the standard deviation (σ), and coefficient of variation (CV). According to [8] and [9] the value of density are into the range of the corresponding for the granite stone, but the porosity is higher than the typical values corresponds to this material (0.5-1.5%). As it is possible to note, the young's modulus obtained with the compression test (6.07 GPa) is lower than these estimated with the Schmidt hammer (7.9–10.6 GPa), but the compression strength (75 MPa) is higher than theses estimated with the Schmidt hammer (23.7–29.8 MPa)

Table 3: Results of the laboratory test of all the samples

N°	Property	Units	Average	σ	CV [%]
1	Volumetric density (ρ)	[kg/m^3]	2595	182	7.03
2	Apparent density (ρ)	[kg/m^3]	2518	24	0.96
3	Porosity	[%]	4.82	0.96	19.99
4	Absorption	[%]	1.92	0.4	20.85
5	Ultrasonic test (vp)	[m/s]	2058	510	24.76
6	Compression strength (fc)	[MPa]	75	10	13.63
7	Young modulus (E)	[MPa]	6074	1129	18.58

6 Conclusions

Based on inspection and diagnosis of the monastery, it was observed that the deterioration of the building might be mainly associated with environmental factors, hence it is recommendable to take measures to protect the monastery. In this sense, the construction of a roof structure to protect the building from water infiltration is of highest importance.

The compressive strength of the stone obtained using correlations and results from Schmidt Hammer were notably lower than the results from the compression tests performed on laboratory (less than the half). This would suggest that the correlation used to estimate the strength in this case was not adequate. In this sense, it would

recommendable to use the values of the laboratory tests, given that the values are similar to the characteristic of the granite stone of the north of Portugal. However, the Young's modulus obtained by both methods was approximate, being the difference around 35%. These results might be applied to define the properties of elements such as stone lintels and the columns of the arcade of the monastery when developing a numerical model.

The three types of walls identified in this study evidence the constructive stages throughout its history. Based on the MQI index and sonic test, it results clear that the quality of the masonry in each sector is different, therefore, this characteristic must be taken into consideration when performing the structural analysis. The sonic tests indicate that M3 walls present the best quality (MQI = 9.5), also in this wall the Young's modulus was high (E = 2300 MPa), hence it is expected that it presents a good behavior to vertical loads. On the other hand, masonry type M1 has the lowest values of MQI (2.5) and Young's modulus of 1560 MPa, therefore, the performance might not be adequate when supporting vertical loads. Finally, the results obtained from the sonic tests might be used to define the properties of the walls in a structural analysis software for a static and dynamic evaluation.

7 Acknowledgements

The authors would like to acknowledge to the ELARCH (Euro-Latin America partnership in natural Risk mitigation and protection of the Cultural Heritage) for funding the postgraduate studies of the first four authors of this paper, and additionally to Saulo Lopez and Eduardo Ramirez for their invaluable assistance in the development of this paper.

8 References

[1] Sistema de informação para o patrimonio arquitectónico, Portugal. (2017). http://www.monumentos.gov.pt/Site/APP_PagesUser/SIPA.aspx?id=3604. Accessed 30 april 2017.
[2] Vergès-Belmin, V. (2010). *Illustrated glossary on Stone deterioration patterns. English-French Ed. Monuments & Sites 15*. International Scientific Committee for Stone. https://www.icomos.org/publications/monuments_and_sites/15/pdf/Monuments_and_Sites_15_ISCS_Glossary_Stone.pdf.
[3] Borri A, Castori G, Corradi M, De Maria A (2015) A method for the analysis and classification of historic masonry. Bull Earthquake Eng. 13:2647–2665.
[4] Suárez L (2014) Estimación de la variabilidad mecánica de placas de roca por ensayos no-destructivos. Ingenieria y Ciencia, Vol. 10, no. 19, pp. 221–246.
[5] Aydin a, (2009). ISRM Suggested method for determination of the Schmidt hammer rebound hardness:Revised version. International Journal of Rock Mechanics & Mining Sciences 46. 627–634.
[6] O. Katza, Z. Rechesa, J.-C. Roegiers (2000). Evaluation of mechanical rock properties using a Schmidt Hammer. International Journal of Rock Mechanics and Mining Sciences 37 (2000) 723-728.
[7] Ministerio delle Infraestrutture e dei Transporti Ministerial Decree dated of 14-01-2008. (2008). NTC. Norme techniche per le construzione. Rome. [In Italian].
[8] S. E. Chidiac and S. Food (2002), Guidelines for the seismic assessment of stone-masonry structures. Quebéc-Canada.
[9] G. Vasconcelos. (2005). "Experimental investigations on the mechanics of stone masonry: characterization of granites and behavior of ancient masonry shear walls, PhD Thesis," University of Minho, Portugal.